

X-Ray Spectroscopy & Moseley's Law*

Craig Reingold[†]

*Department of Physics,
The University of Notre Dame*

Patricia Huestis[‡] and Shane Moylan[§]

*Department of Physics,
The University of Notre Dame*

(Experimental Methods in Physics, Spring 2016)

(Dated: February 29, 2016)

X-Ray fluorescence is a precise and reliable method of determining the elemental composition of a material. In this work, we were able to demonstrate the reliability of this method by bombarding various materials with x-rays, thus forcing the material to fluoresce x-rays characteristic of the elemental composition of the material. Comparing the measured x-rays to known x-ray energies allowed us to accurately predict the elemental composition of various materials, such as pyrite, gold foil, bismuth and germanium crystals, and pennies from various countries.

We were also able to use the K_α lines seen from these fluorescing sources to verify Moseley's law. Moseley's law is an empirically derived formula that relates the frequency of an x-ray to the square of the proton number of the atom the x-ray originated from. Moseley's law contains two empirically derived constants, $k_1 = 4.97 \cdot 10^7$ and $k_2 = 1$. We were able to measure these constants as $k_1 = (5.04 \pm 0.15) \cdot 10^7$ and $k_2 = 1.32 \pm 0.89$, allowing us to confirm Moseley's law experimentally.

I. INTRODUCTION & THEORY

A. X-Ray Fluorescence

Photons interact with atoms electromagnetically. For photons with lower energies than γ -rays, these interactions typically occur with the electrons in the atom. For photons within the x-ray energy range, the photon will have enough energy to liberate one of the electrons in the inner shells of the atom via the photoelectric effect. This configuration is not energetically favorable, and so the electrons rearrange themselves into a more favorable configuration. This rearrangement typically involves an electron from a higher orbital transitioning to the position the ejected electron previously occupied. A cartoon representation of this process can be found in FIG. 1

As the electron transition from a higher energy to lower energy orbital, it releases its excess energy as a photon. The emitted photon is also in the x-ray energy range. Due to the quantum mechanical nature of the electron orbital configurations, the possible x-ray energies are characteristic of the element they originated from, as well as of the initial and final orbital location. A level scheme for the possible transitions, and the names associated with each transition can be found in

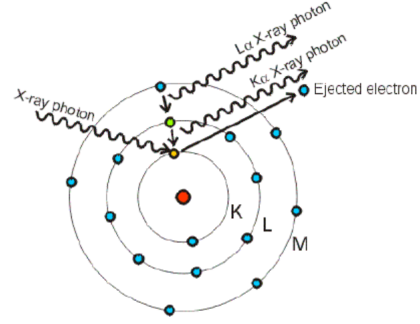


FIG. 1. An illustration of the process by which x-rays fluoresce from a material. An incident x-ray liberates an electron from the atom. An electron from a higher energy shell falls to a lower energy shell to take the place of the liberated electron, and in the process, emits a new, characteristic x-ray.

FIG. 2.

B. Moseley's Law

Moseley's law is an empirically derived equation [3]. Moseley's law for K_α transitions can be found in EQN. 1.

$$f(K_\alpha) = (k_1)^2 \cdot (Z + k_2)^2 \quad (1)$$

$$k_1 = 4.97 \cdot 10^7 \quad k_2 = 1$$

* from *Advanced Physics Laboratory Manual*, [1]

[†] Primary Author, NSH 284, creingol@nd.edu

[‡] NDRL 316, phuestis@nd.edu

[§] NSH 284, smoylan1@nd.edu

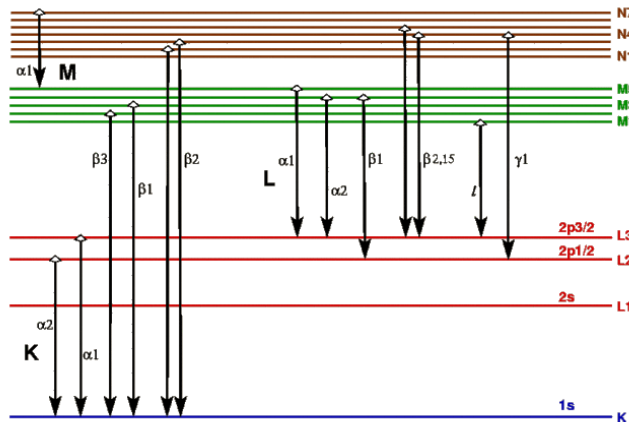


FIG. 2. A level scheme correlating x-ray types with the appropriate transition between electron orbitals [2]. As seen above, K_{α} x-rays correspond to an electron transitioning from the p -orbital to the s -orbital. K_{β} x-rays correspond to an electron transitioning from the d -orbital to the s -orbital.

The Z in EQN. 1 is the number of protons in the atom, and the other constants have been derived empirically. In this work, we will attempt to remeasure these constants.

II. EXPERIMENTAL SETUP

A. Apparatus

The block diagram of our experimental setup can be found in FIG 3. The Si(Li)-detector from this experiment was operated at LN_2 temperatures throughout the entire experiment. The detector was calibrated using a variable energy source (FIG. 4). The variable energy source was actually six different foils, Tb, Rb, Mo, Ag, Cu, and Ba, placed over an ^{241}Am source. As the ^{241}Am source α -decayed, the emitted α would interact with the foils, causing them to emit x-rays.

After calibration, we bombarded seven materials that did not radiate x-rays naturally with photons from our x-ray tube. The sources used can be found in TABLE I.

B. Procedure

A variable energy source was used to calibrate our Si(Li)-detector. The energies of the photons emitted by the calibration sources are well known. Gaussian probability distributions were fit to each of the signals seen in the detector [4]. The mean of each of these fits was plotted against the expected energy of photon corresponding to a transition in the source. The standard deviation of the fit was used as the uncertainty. A first order polynomial was then fit to the plot of energy

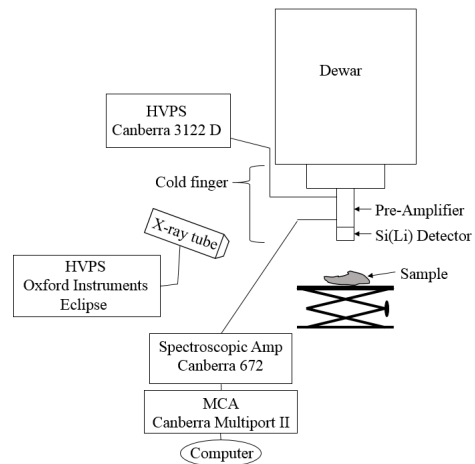


FIG. 3. This is a block diagram of our experimental setup. A lithium-drifted silicon semiconductor detector was placed over our sample to detect x-rays. Data taken with our detector was sent through a spectroscopic amplifier, and then through a Multi-Channel Analyzer (MCA) that was able to bin and digitize the signal. Our detector was calibrated with a variable energy source (FIG. 4). For the other sources not contained within our variable energy source, the x-ray tube was used to generate a beam of x-rays to force the sources to fluoresce x-rays.

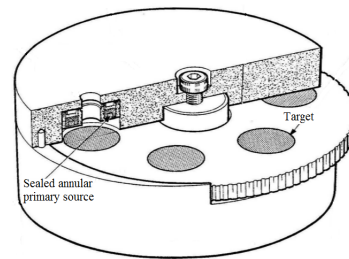


FIG. 4. A schematic of our variable energy x-ray source. On the inside, there is a disk with six different foils. The foils were Ag, Ba, Cu, Mo, Rb, and Tb. This disk is encased in a shielding material, with a small aperture in the top, surrounded by a ^{241}Am source. The aperture allowed us to collimate the x-ray beam emitted from the foils after they were excited by the α -particle emitted from the ^{241}Am source, and to select only one x-ray source at a time. The x-ray source was selected by rotating the inner disk.

versus channel [5]. The result of this fit was then used as the linear calibration.

After calibration, seven sources of unknown¹ elemental composition were bombarded with photons from the x-ray tube. These x-rays liberated an electron from the

¹ The composition of our sources was not actually unknown. For example, the composition of the coins used in this paper is well documented by the countries the coins were minted in.

material, and the photon released from the subsequent transition was measured in our Si(Li)-detector. The measured peaks for each material were fit to Gaussian functions, with the mean of the fit corresponding to the energy of the fluoresced photon. These energies were then compared to known x-ray energies [2] to determine the elemental composition of the material.

It is obvious that if EQN. 1 is taken to the $\frac{1}{2}$ power, it becomes a first order polynomial in Z . Therefore, to confirm Moseley's law, we were able to plot the square root of the frequency of our measured K_α lines against the number of protons in the corresponding element, and fit this plot to a first order polynomial. The fit parameters from this regression allowed us to confirm the constants k_1 and k_2 cited in Moseley's Law.

III. DATA & ANALYSIS

A. Data

Our calibration data can be found in FIG. 6. The measured and theoretical energies of the fluoresced x-rays can be found in TABLE II

B. Analysis

In order to determine the centroid of each peak in our analysis, we fit Gaussian distributions to the data. The mean and standard deviation from the fit were used as the energy of the x-ray, and uncertainty in the energy respectively.

We were able to determine the actual E_γ found in TABLE II using a software called Hephaestus [2]. This, in combination with knowing the rough composition of some of the sources [6-8], allowed us to identify the elemental composition of each of the unknown sources.

In order to confirm Moseley's law, we plotted the square root of the K_α x-ray frequency from TABLE II against the number of protons in each source. The results of this plot, and the linear fit of our data, can be found in FIG. 5. It is evident, from our figure, that the fitting a first order polynomial to the data was appropriate.

IV. DISCUSSION

After seeing the data recorded in FIG. 6, it is clear we were able to easily obtain a linear calibration. The linear calibration was facilitated by the number of peaks we were able to see in this figure, the high

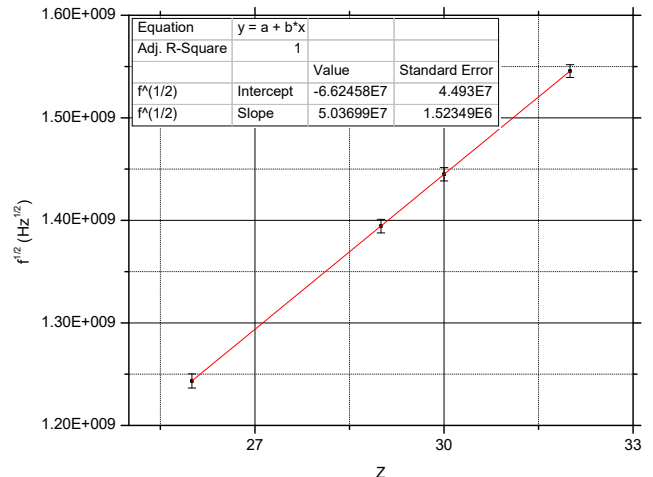


FIG. 5. A plot of the square-root of photon frequency as a function of proton number. From these fit results, we determined our experimental values of the Moseley's law constants to be $k_1 = (5.04 \pm 0.15) \cdot 10^7$ and $k_2 = 1.32 \pm 0.89$

signal to background ratio, and the clear separation of most of the peaks. While there are clearly doublets in FIG. 6 for sources such as Tb, they were easily dealt with by fitting a linear combination of two Gaussian functions simultaneously instead of fitting two different, independent Gaussians.

After calibration, we were tasked with determining the composition of each of our unknown sources. This task was facilitated by spectroscopy software [2], however, we still ran into a few peculiarities. First, we were able to see low energy x-rays in some of the data that did not seem to correspond with anything in the fluorescing x-ray source. While we were unable to identify the source of these x-rays, the most probable source of these low energy x-rays was the stand on which the sources were placed. Given the small size of some of our sources, and the rudimentary method of aiming the x-rays produced by the x-ray tube, it is incredibly possible that along with bombarding our intended target, we were also bombarding the stand with x-rays, causing materials inside the stand to emit x-rays.

Second, we were also unable to correctly identify the elemental composition of the Canadian penny. According to the Canadian mint [7], the pennies minted in 1982 should be composed of Cu, Sn, and Zn (TABLE I). Our findings, however, suggest that the coin we placed under our beam contained Cu and Fe, one of the primary components of steel. Copper plates steel pennies were not minted in Canada until much later. Our current assumption is that we misread the coin, and that it was not in fact minted in 1982. There is no mistaking the two

x-rays seen in our spectrum with Sn and Zn, they are absolutely lines emitted from transitioning electrons in Fe

Referring to FIG. 5, the accepted values of k_1 and k_2 are both within one standard deviation of our calculated values. Therefore, our confirmation of Moseley's law for

K_α x-rays was successful. There are other constants associated with Moseley's law for different x-rays, such as K_β , L_α , etc. However, we were unable to see enough lines of any other type (TABLE II) to reliably calculate these constants.

-
- [1] J. Hammer, *Advanced Physics Laboratory Manual* (Department of Physics, University of Notre Dame, 2008).
 - [2] B. Ravel and M. Newville, *Journal of Synchrotron Radiation* **12**, 537 (2005).
 - [3] H. Moseley, *Philosophical Magazine* **1024** (1913).
 - [4] OriginLab, *OriginPro 8.0* (2007).
 - [5] R. Brun and F. Rademakers, *Nucl. Inst. & Meth. in Phys. Res. A* **389**.
 - [6] U. S. Mint, *The Composition of the Cent* (2016).
 - [7] R. C. Mint, *A national symbolthe 1-cent coin* (2016).
 - [8] T. R. Mint, *One Penny Coin* (2016).

V. APPENDIX

Sample	Composition	$K_{\alpha 1}$ (keV)	$K_{\beta 1}$ (keV)	$L_{\alpha 1}$ (keV)	$L_{\beta 1}$ (keV)
Pyrite	42% Fe	6.40	7.06	-	-
	58% S	1.74	1.83	-	-
Gold foil	Au	-	-	9.71	11.44
Bismuth	Bi	-	-	10.84	13.02
US penny (2009) [6]	97.5% Zn	8.64	9.57	-	-
	2.5% Cu	8.05	8.90	-	-
Canadian penny [7] (1986)	98% Cu	8.05	8.90	-	-
	1.75% Sn	-	-	3.44	3.66
	0.25% Zn	8.64	9.57	-	-
British penny [8] (1993)	Cu plated	8.05	8.90	-	-
	Fe (steel)	6.40	7.06	-	-
Glossy rock	Unknown	-	-	-	-

TABLE I. Samples used for x-ray fluorescence. Not all materials present in the sample give noticeable x-ray lines. Peaks that are out of the range of the detector are not given in this table.

Calibration

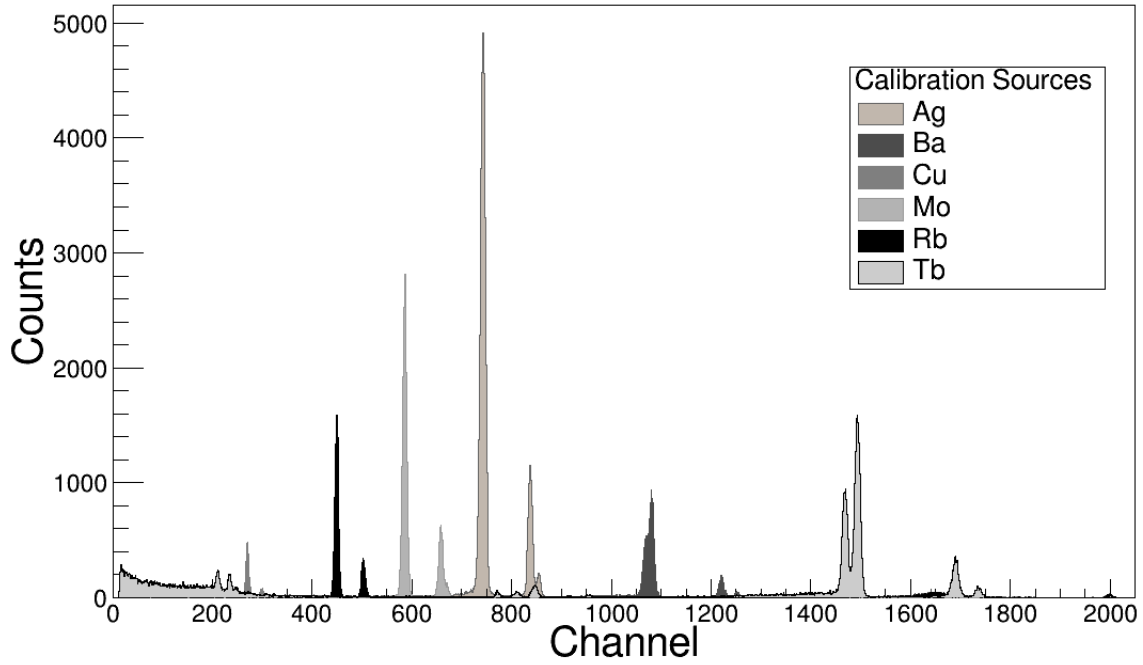


FIG. 6. Data measured with our Si(Li)-detector for each of the radioactive sources in our variable energy source, superimposed on top of each other.

Sample	Measured peak (keV)	Accepted peak (keV)	Measured peak (keV)	Accepted peak (keV)
Pyrite	6.394 ± 0.071	6.40	7.048 ± 0.076	7.06
Gold foil	9.709 ± 0.085	9.71	11.485 ± 0.115	11.44
	13.376 ± 0.086	13.38	13.739 ± 0.141	13.71
Bismuth	10.834 ± 0.881	10.84	13.023 ± 0.099	13.02
	15.254 ± 0.121	15.25	15.698 ± 0.096	15.71
US penny	8.042 ± 0.076	8.05	8.634 ± 0.078	8.64
	8.914 ± 0.073	8.90	9.576 ± 0.085	9.57
Canadian penny	8.044 ± 0.075	8.05	8.896 ± 0.086	8.90
British penny	8.043 ± 0.178	8.05	8.905 ± 0.079	8.90
Germanium ^a	9.879 ± 0.079	9.89	10.983 ± 0.085	10.98

^a The last sample in table 1 was originally unknown. The energy peaks along with the sample's appearance helped identify the sample as germanium.

TABLE II. Measured x-ray centroids in keV from each of the materials we exposed to our x-ray beam, and the accepted value for the characteristic x-ray energy.